Materials Physics and Mechanics. 2023;51(3): 66-74
Research article
http://dx.doi.org/10.18149/MPM.5132023_9

Submitted: September 13, 2022
Approved: February 7, 2023
Accepted: May 15, 2023

Influences of multi-walled carbon nanotubes incorporated into poly(methyl methacrylate-co-acrylic acid)/polyethylene glycol

G.Q. Liu ✉, M.Y. Hou, S.Q. Wang

Henan University of Technology, Zhengzhou, China

✉ polymerpaper@163.com

Abstract. In this article, by ultrasonic-assisted dispersion of poly(ethylene glycol) (PEG) and multiwalled carbon nanotubes (MWCNTs), methyl methacrylate (MMA) and acrylic acid (AA) are copolymerized and crosslinked through in situ radical bulk polymerization, namely fabricating P(MMA-co-AA)/PEG/MWCNTs composites. The influences of MWCNTs contents in morphology, thermal and mechanical properties of the composites are investigated. After treated by mixed acid, MWCNTs can be uniformly dispersed in P(MMA-co-AA)/PEG due to the hydrogen bonding. Compared with P(MMA-co-AA)/PEG, both the glass transition temperature and the degradation temperature of the composites increase with increasing content, and increase at least 7 and 13 °C, respectively; their tensile strength and impact strength at least increase 9 and 65 %, respectively, and the elongation at break is reduced by at least 8 %.
Keywords: composites, thermal and mechanical properties, storage modulus

Acknowledgements. *Financial support from the Science and Technology Project of Henan Province (No. 172102210033).*

Citation: Liu GQ, Hou MY, Wang SQ. Influences of Multi-walled Carbon Nanotubes Incorporated into Poly(methyl methacrylate-co-acrylic acid)/polyethylene glycol. *Materials Physics and Mechanics.* 2023;51(3): 66-74. DOI: 10.18149/MPM.5132023_9.

Introduction

Polymer-based composites exhibit extremely superior performance compared to pure polymers [1–6]. Among them, polymers composites with carbon nanotubes (CNTs) are the most widely investigated. Adding CNTs to polymers, even a very small amount, can clearly improve polymer properties, for example, strength and heat resistance. So, CNTs are often used as nanofillers for fabricating polymer-based nanocomposites [7–11], and mainly include single-wall carbon nanotubes (SWCNTs) and MWCNTs. The former is widely studied due to its unique one-dimensional structure with strong mechanical properties and adjustable electric conductivity. The latter, in contrast with SWCNTs, is lower unit cost, and relatively easier dispersion. Although the addition amount of SWCNTs is much lower than that of MWCNTs and makes materials' properties enhance even further, MWCNTs are still diffusely chosen.

PMMA has wide application in many fields, including signal light equipment, denture base materials, etc. Its high transparency, good biocompatibility, easy processing and low cost can better reflect its advantages in practical applications. Although PMMA is still widely used in all walks of life, it still has its own inherent problems, for example, its weak mechanical properties. Therefore, there are many attempts of modifying PMMA to expand its application. PMMA's modification methods include blending modification [12,13], chemical modification [14,15], filling and fiber enhancement modification [16,17], surface modification [18,19], and composite modification [20–22], and so on. Among them, the compounding of PMMA is

Publisher: Peter the Great St. Petersburg Polytechnic University

undoubtedly a commonly used method for improving its performance, especially the composites of nano-filler and PMMA, such as graphene oxide[20,23,24], TiO_2 [21], CNTs [22,25], ZnO [26], $BaTiO_3$ [27], nanofibers [28], etc. These nanoparticles introduced to PMMA improve the performance of the composites from all aspects [20–30].

So far, the modification of PMMA has been carried out to meet its growing application requirements. Most of the work pays attention to the improvement of PMMA's modification and their mechanical properties. However, there are few researches on the preparation of PMMA-based composite by MMA co-polymerization and blending polymer.

In this study, in order to combine good adhesion and high mechanical strength, AA is selected as a copolymer component. Owing to its good biocompatibility coupled with a dual-role as both plasticizer and dispersant, PEG, which can also adjust the glass transition temperature of the composite, and MWCNTs as reinforcing fillers, are incorporated into P(MMA-co-AA). These composites can be prospective to display widely potential application in bone cements.

This research is dedicated to preparing PMMA blend composites through in situ polymerization, simplifying the preparation process, and obtaining its composites with improved performance.

Experiment

MWCNTs were bought from Shenzhen Nanotech Port (China). AIBN, MMA and AA were from Chengdu Kelong Chemical Co., Ltd (China). AIBN was an initiator and purified by recrystallization. Prior to polymerization, MMA and AA were separately vacuum-distilled so as to refine monomer. Cross-linker EGDMA (Aldrich) and PEG (Aldrich, Mn=4000) were used as received.

Firstly, 150 ml of 1:3 (v/v) HNO_3/H_2SO_4 mixtures soaked 2 g MWCNTs and refluxed for 8 hours. Then, the acid-treated MWCNTs (a-MWCNTs) were washed with deionized water till neutral and dried by vacuum at 85 °C. During the polymerization reaction, the contents of MMA and AA remained 1:1 (v/v) with changes in those of a-MWCNTs. Firstly, the same volume content of MMA and AA, PEG (21 wt.% relatively to the mass of the entire monomers (MM)), AIBN (0.5 wt.% of MM), EGDMA (5 wt.% of MM) and a-MWCNTs (Its addition was 0.5, 1.0, 1.5 and 2.0 wt.% of MM, respectively) were added into a three-necked flask (100 ml); they were sonicated for 30 minutes, bubbled with N_2 to remove O_2, rapidly warmed to 70 °C, proceeded to sonicate and stir for 30 minutes, afterward lowered temperature from 70 to 55 °C, and polymerized 24 hours. Finally, P(MMA-co-AA)/PEG/MWCNTs composites were fabricated and dried under vacuum at 80 °C 24 hours.

Fourier transform infrared spectra (FTIR 8300PCS, Shimadzu) could characterize the specific functional groups. The fractured surface was examined with scanning electron microscope (SEM, JSM-5900LV). The dynamic mechanical analysis (DMA) were performed on the Du Pont 983 instrument. A differential scanning calorimeter (DSC, DuPont 9900) and a thermogravimetric analysis (TGA, Perkin-Elmer) were used. The notched Izod impact strength was measured with XJ-40A pendulum apparatus (China).

Result and Discussion

The functional groups of MWCNTs, a-MWCNTs, P(MMA-co-AA)/PEG and their composites are characterized in Fig. 1. After treated by H_2SO_4/HNO_3, the defect of MWCNTs increases, which helps them oxidation to form a lot of oxygen-containing functionalities, *i.e.*, carboxyl (-COOH) or hydroxy (-OH) [31,32]. Compared a-MWCNTs with MWCNTs, the -COOH and -OH groups can be found to be attached on a-MWCNTs surface. The FTIR of a-MWCNTs shows a wide peak at 3435 cm^{-1}, in correspondence to -OH; the -COOH and carbonyl (>C=O) groups correspond to the peak at 1723 cm^{-1}. Acid treatments of MWCNTs not only remove

impurities in them, but also partially oxidize carbon, which undoubtedly helps to form more functional groups on MWCNTs. The C=C and hexagonal carbon, respectively, in the lowering peak regions of 1534 cm^{-1}, and in 500 - 1000 cm^{-1} regions, are oxidized. Declining peak intensity indicates the existence of a great deal of asymmetric hexagonal carbon. Likewise, after mixed acid handling, >C=O of quinoid unit on CNTs has a pointed peak centered 1647 cm^{-1}, whose peak intensity is also weakened. The above results show that there are some -COOH formed on the surface of MWCNTs.

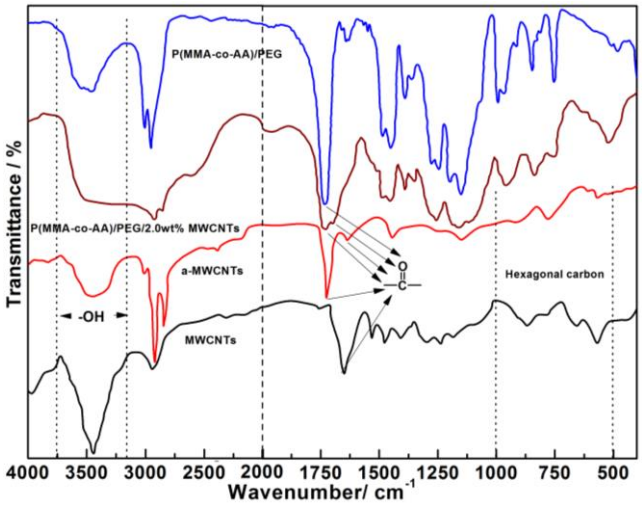

Fig. 1. FTIR of MWCNTs, a-MWCNTs, P(MMA-co-AA)/PEG and the composites

Since the interaction between -OH and >C=O may form a hydrogen bond, their regions of stretching vibrations, namely 3157-3752 and 1697-1736 cm^{-1}, have to be paid to attention in Fig. 1. In contrast with P(MMA-co-AA)/PEG, the >C=O peak in P(MMA-co-AA)/PEG/MWCNTs is divided into two peaks at 1700 and 1729 cm^{-1}, which are hydrogen-bonded carbonyl and free carbonyl peaks. Similarly, due to the participation of some hydroxyl groups in the formation of hydrogen bonds, the hydroxyl group of P(MMA-co-AA)/PEG/MWCNTs has a broad peak at 3355 cm^{-1}, and that of P(MMA-co-AA)/PEG shows a relatively narrow peak at 3513 cm^{-1}. The reason is that the hydrogen bonds exist between P(MMA-co-AA)/PEG and a-MWCNTs, *i.e.*, hydroxyl-carbonyl interaction between them, and undoubtedly promote the dispersion of a-MWCNTs in P(MMA-co-AA)/PEG.

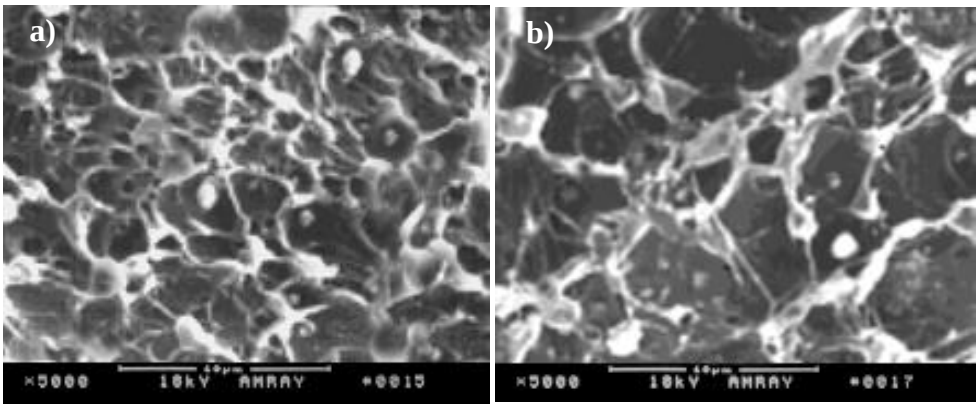

Fig. 2. SEM images of P(MMA-co-AA)/PEG/MWCNTs fracture surfaces: (a) 0.5 wt.% MWCNTs, (b) 2.0 wt.% MWCNTs

The homogeneous dispersion of MWCNTs in polymer plays a key role in their reinforcing effects. The FTIR analysis has shown that there is an interaction between P(MMA-co-AA)/PEG and a-MWCNTs, which can increase their miscibility. SEM can be used to observe the dispersed state of a-MWCNTs in P(MMA-co-AA)/PEG. Figure 2 shows the fracture surfaces of P(MMA-co-AA)/PEG/MWCNTs composites. It can be observed that a-MWCNTs are uniformly dispersed in the composites.

Some a-MWCNTs are pulled out with one end still powerfully embedding in P(MMA-co-AA)/PEG like an 'anchor'; meanwhile, there are some holes left due to a-MWCNTs pulling out of P(MMA-co-AA)/PEG. Both a-MWCNTs and the holes are evenly distributed and no agglomeration of a-MWCNTs is found. This means that there is an interaction between a-MWCNTs and P(MMA-co-AA)/PEG, that is, hydrogen bonds interaction between them, as shown in FTIR analysis, thereby promoting the dispersion of a-MWCNTs.

The influences of MWCNTs contents in the glass transition temperature (T_g) is shown in Fig. 3. Obviously, the T_g of all P(MMA-co-AA)/PEG/MWCNTs composites is higher than that of P(MMA-co-AA)/PEG. T_g of P(MMA-co-AA)/PEG is 67 °C and that of the composites is 74, 77, 80 and 83 °C, separately, increasing with MWCNTs content; the higher T_g is ascribed to the homogeneous dispersion of rigid MWCNTs in polymer matrices and the hydrogen bonds between MWCNTs and P(MMA-co-AA)/PEG, which can considerably constrict the motion of polymeric chain segments and increase the T_gs of P(MMA-co-AA)/PEG/MWCNTs composites. Those also confirm the analysis results of FTIR and SEM.

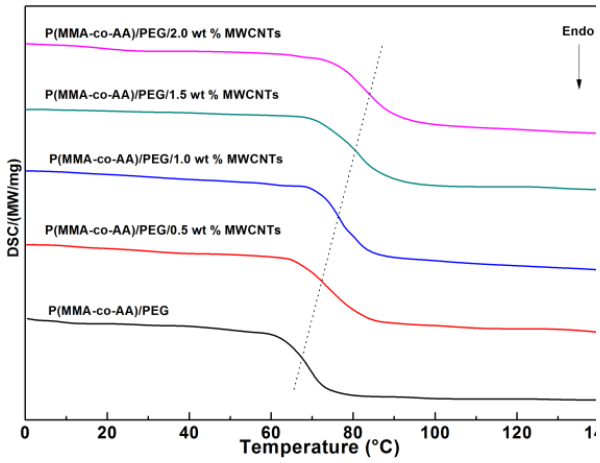

Fig. 3. DSC of P(MMA-co-AA)/PEG and the composites

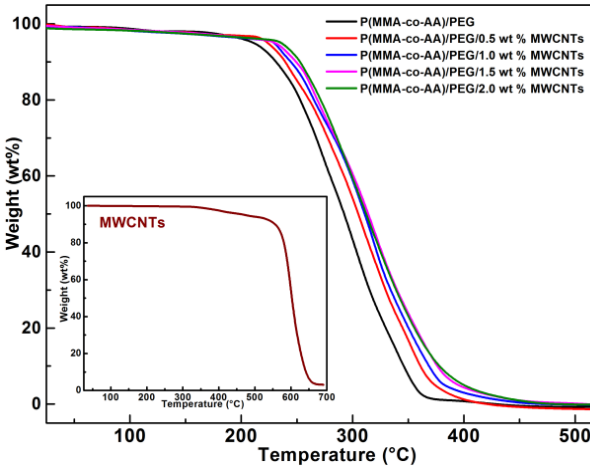

Fig. 4. TGA curves of MWCNTs, P(MMA-co-AA)/PEG and their composites

The influences of MWCNTs contents in the thermal stabilities are measured by TGA, as displayed in Fig. 4. The 5 % weight loss temperature is defined as degradation temperature (T_d). Apparently, the incorporation MWCNTs into P(MMA-co-AA)/PEG improves its thermal stability. T_d of the composites is not less than 13 °C higher than that of P(MMA-co-AA)/PEG, which stems from the contribution of MWCNTs. The uniformly dispersed MWCNTs can stop the releasing of thermally degraded small-molecules gases and slow the composites thermal degradation, which makes the composites degrade much more slowly than P(MMA-co-AA)/PEG. At 337 °C, the thermal degradation residues of P(MMA-co-AA)/PEG are only 15 wt%, whereas those of the composites remain ca. 25-32 wt.%, as shown in Fig. 4, indicating their composites thermal stabilities are improved after MWCNTs are incorporated into P(MMA-co-AA)/PEG.

Figure 5 is E'-temperature curves of P(MMA-co-AA)/PEG and its composites, which shows MWCNTs can play a part in reinforcement agents and the higher the contents of

MWCNTs, the more significant its reinforcing effect. *E´* can represent the viscoelastic materials' stiffness and proportional to the energy stored. When the temperature decreases, the motion of the polymer is 'frozen' and thus the polymer remains rigid, which restricts the motion of the macromolecular segments with no shape change, especially when rotating around C-C. With increasing temperature, the movement of polymeric segments is easier and easier, and easily responds to the loading. Their slipping and untangling occasionally occur, even though the strong entanglement is still maintained between the macromolecules.

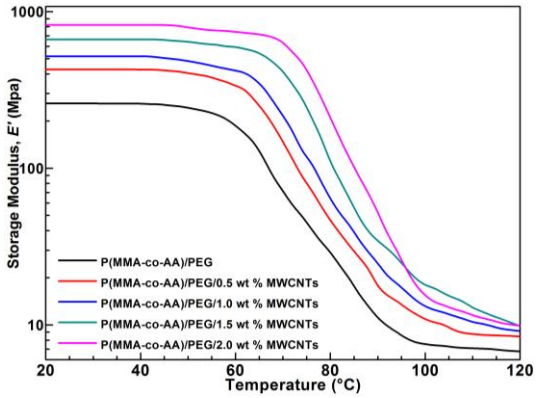

Fig. 5. Storage modulus (*E´*) of P(MMA-co-AA)/PEG and the composites

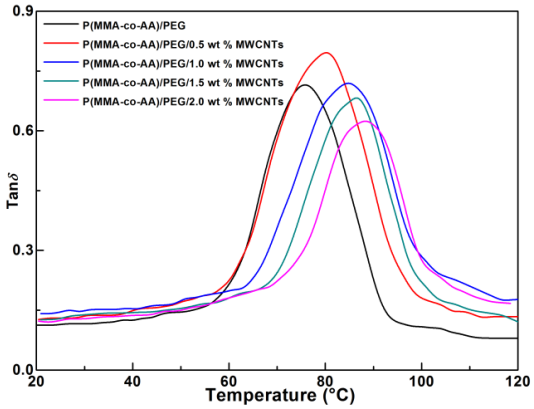

Fig. 6. Loss factor (*tanδ*) peaks of P(MMA-co-AA)/PEG and the composites

At 20 °C, P(MMA-co-AA)/PEG shows a value of *E'* = 260 MPa in Fig. 5; while in P(MMA-co-AA)/PEG with 0.5, 1.0, 1.5 and 2.0 wt.% of MWCNTs, the corresponding *E'*s are 427, 518, 664 and 822 MPa, separately; the respective *E'*s are 11.10, 17.63, 24.86, 34.44 and 51.52 MPa at 90 °C. In comparison with P(MMA-co-AA)/PEG, these results show a relevant *E'* rise in P(MMA-co-AA)/PEG/MWCNTs and indicate an increment in *E'* of at least 64.2 % at 20 °C, and at 90 °C, *E'* of P(MMA-co-AA)/PEG/MWCNTs composites is over 3.6 times higher than that of P(MMA-co-AA)/PEG, which seems that the polymer chains are effectively immobilized by the MWCNTs, and therefore, the composite has a higher *E'*. Obviously, the initial *E'* increases with increasing MWCNTs contents. The MWCNTs enhancement effects origin from its inherent stiffness and its 'anchor' effect on macromolecular chains.

*Tanδ*s of P(MMA-co-AA)/PEG and the composites are shown in Fig. 6. Usually, the temperature corresponding to the maximum peak is deemed as T_g. As the content of MWCNTs increases, the temperature corresponding to *tanδ* peak shows an increasing trend, that is, T_g increases. Compared with T_g of P(MMA-co-AA)/PEG, that of the composites is increased by a minimum of 6 °C, which shows that MWCNTs are uniformly dispersed in the polymers and restrict the macromolecular chains motion. On the other hand, the hydrogen bonds between the polymer and MWCNTs can act as physical cross-linking, which reduces the polymer chain mobility and leads to a gradual increase in T_g.

The influence of MWCNTs content in Izod impact strength is displayed in Fig. 7. The addition of MWCNTs has a significant effect on the impact strength. Compared with the impact strength of P(MMA-co-AA)/PEG, When the addition of MWCNTs is 0.5 wt.%, that of the composite increases by 65 %; as MWCNTs exceeds 1.0 wt.%, the increasing trend of the impact strength slows down; while MWCNTs is 2.0 wt.%, there is not much increase. The test results indirectly reflect the uniform dispersion of MWCNTs in the polymer, thus improving its impact strength. The reasons can be summed up as follows: both MWCNTs and the hydrogen bonds in the composites play the role of physical cross-linking. Because its formation is reversible, the physical cross-linking can improve the impact strength of the composites.

Figure 8 shows the tensile strength of P(MMA-co-AA)/PEG and the composites. Obviously, introducing MWCNTs into a polymer can increase its tensile strength. With increasing MWCNTs contents, their tensile strength raises 9% as the MWCNTs content of 0.5 wt.%. When MWCNTs content reaches 3.0 wt.%, the strength increases by 28 %. This can be interpreted as the enhancement effects of MWCNTs, like the previous impact strength analysis.

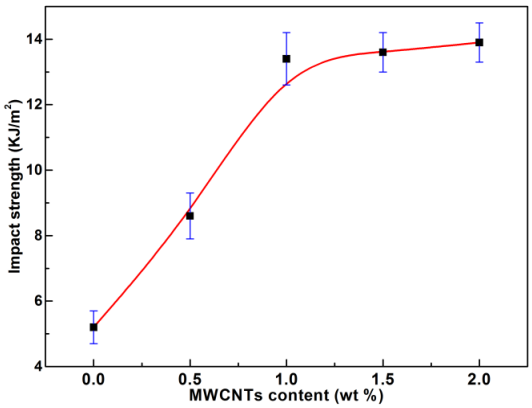

Fig. 7. Impact strength of P(MMA-co-AA)/PEG and the composites

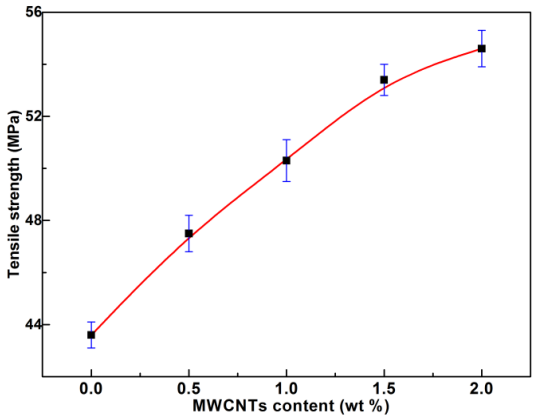

Fig. 8. Tensile strength of P(MMA-co-AA)/PEG and the composites

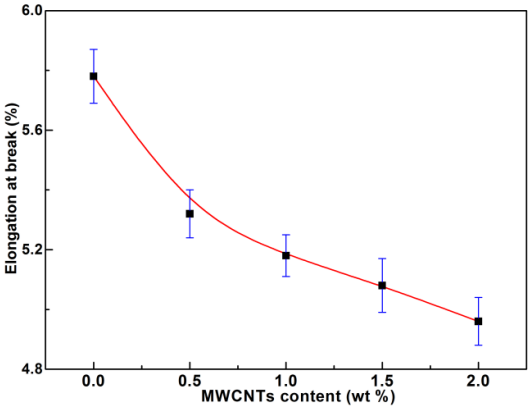

Fig. 9. Elongation at break of P(MMA-co-AA)/PEG and the composites

Figure 9 shows the elongation at break of P(MMA-co-AA)/PEG and the composites. Apparently, the introducing of MWCNTs can increase the stiffness of polymer matrix and restrict chain segments motion, which makes materials less ductile. In comparison with P(MMA-co-AA)/PEG, the elongation at break of the composite with 3 wt.% MWCNTs is reduced by 15 %. The rigidity of MWCNTs and the hydrogen bonds existing in the composites analyzed above can inhibit the movement of polymer chains, thus increasing brittleness and reducing ductility.

All in all, compared with P(MMA-co-AA)/PEG, with the increase of MWCNTs content, the mechanical properties of the P(MMA-co-AA)/PEG/MWCNTs composites have changed significantly, that is, initial *E´*, tensile and impact strength of the composites increase, but their elongation at break decrease, indicating that the P(MMA-co-AA)/PEG/MWCNTs composites present hard and strong properties.

Conclusions

Compared with P(MMA-co-AA)/PEG, modification of the P(MMA-co-AA)/PEG blends with the a-MWCNTs (up to 2 wt.%) can improve their performance. Owing to a-MWCNTs uniformly dispersed in P(MMA-co-AA)/PEG, T_g, T_d and initial E' of the composites increase with a-MWCNTs content increasing; their tensile and impact strength are also improved to a certain extent; however, the elongation at break of the composite shows a decreasing trend.

Investigation of a-MWCNTs shows that there are some -COOH formed on the surface of MWCNTs after mixed acid treatment, there are some hydrogen bonds exist between P(MMA-co-AA)/PEG and a-MWCNTs.

The polymer modification method is simple and economical. In the process of synthesis of polymers, nanocomposite materials can be made according to the actual requirements.

References

1. Guo Z, Poot AA, Grijpma DW. Advanced polymer-based composites and structures for biomedical applications. *European Polymer Journal*. 2021;149: 110388.
2. Varshney S, Mishra N, Gupta MK. Progress in nanocellulose and its polymer based composites: a review on processing, characterization, and applications. *Polymer Composites*. 2021;42(8): 3660-3686.
3. Lee JKY, Chen N, Peng S, Li L, Tian L, Thakor N, Ramakrishna S. Polymer-based composites by electrospinning: Preparation & functionalization with nanocarbons. *Progress in Polymer Science*. 2018;86: 40-84.
4. Zhang Y, Josien L, Salomon JP, Simon-Masseron A, Lalevée J. Photopolymerization of Zeolite/Polymer-Based Composites: Toward 3D and 4D Printing Applications. *ACS Applied Polymer Materials*. 2020;3(1): 400-409.
5. Yusupov K, Vomiero A. Polymer-based low-temperature thermoelectric composites. *Advanced Functional Materials*. 2020;30(52): 2002015.
6. Li YM, Deng C, Shi XH, Xu BR, Chen H, Wang YZ. Simultaneously improved flame retardance and ceramifiable properties of polymer-based composites via the formed crystalline phase at high temperature. *ACS Applied Materials & Interfaces*. 2019;11(7): 7459-7471.
7. Oseli A, Vesel A, Zagar E, Perse LS. Mechanisms of single-walled carbon nanotube network formation and its configuration in polymer-based nanocomposites. *Macromolecules*. 2021;54(7): 3334-3346.
8. Ma Q, Hao B, Ma PC. In-situ characterization on the fracture behavior of three dimensional polymer nanocomposites reinforced by CNT sponge. *Composites Science and Technology*. 2022;217: 109132.
9. Zhao J, Huang Y, Wang G, Qiao Y, Chen Z, Zhang A, Park CB. Fabrication of outstanding thermal-insulating, mechanical robust and superhydrophobic PP/CNT/sorbitol derivative nanocomposite foams for efficient oil/water separation. *Journal of Hazardous Materials*. 2021;418: 126295.
10. Duan K, He Y, Liao X, Zhang J, Li L, Li X, Liu S, Hu Y, Wang X, Lu Y. A critical role of CNT real volume fraction on nanocomposite modulus. *Carbon*. 2022;189: 395-403.
11. Kaushal A, Singh V. Excellent electromagnetic interference shielding performance of polypropylene/carbon fiber/multiwalled carbon nanotube nanocomposites. *Polymer Composites*. 2022;43(6): 3708-3715.
12. Srinivasan S, Chhatre SS, Mabry, JM, Cohen, RE, McKinley, GH. Solution spraying of poly (methyl methacrylate) blends to fabricate microtextured, superoleophobic surfaces. *Polymer*. 2011;52(14): 3209-3218.
13. Peng G, Zhao X, Zhan Z, Ci S, Wang Q, Liang Y, Zhao M. New crystal structure and discharge efficiency of poly (vinylidene fluoride-hexafluoropropylene)/poly (methyl methacrylate) blend films. *RSC Advances*. 2014;4(32): 16849-16854.

14. Saithai P, Lecomte J, Dubreucq E, Tanrattanakul V. Effects of different epoxidation methods of soybean oil on the characteristics of acrylated epoxidized soybean oil-co-poly (methyl methacrylate) copolymer. *Express Polymer Letters*. 2013;7(11): 910-924.
15. Lee KS, Lee J, Kwak J, Moon HC, Kim JK. Reduction of line edge roughness of polystyrene-block-poly (methyl methacrylate) copolymer nanopatterns by introducing hydrogen bonding at the junction point of two block chains. *ACS applied materials & interfaces*. 2017;9(37): 31245-31251.
16. Vankayalapati GS, Kaplan E, Lallo LM, Victor N, Clemons CM, Considine JM, Turner KT. Toughening Poly (methyl methacrylate) via Reinforcement with Cellulose Nanofibrils. *ACS Applied Polymer Materials*. 2021;3(12): 6102-6110.
17. Alhareb AO, Akil HBM, Ahmad ZAB. Poly (methyl methacrylate) denture base composites enhancement by various combinations of nitrile butadiene rubber/treated ceramic fillers. *Journal of Thermoplastic Composite Materials*. 2017;30(8): 1069-1090.
18. Ozkutlu M, Dilek C, Bayram G. Effects of hollow glass microsphere density and surface modification on the mechanical and thermal properties of poly (methyl methacrylate) syntactic foams. *Composite Structures*. 2018;202: 545-550.
19. Rezaei F, Shokri B, Sharifian M. Atmospheric-pressure DBD plasma-assisted surface modification of polymethyl methacrylate: A study on cell growth/proliferation and antibacterial properties. *Applied Surface Science*. 2016;360: 641-651.
20. Tavakoli M, Bakhtiari SSE, Karbasi S. Incorporation of chitosan/graphene oxide nanocomposite in to the PMMA bone cement: Physical, mechanical and biological evaluation. *International journal of biological macromolecules*. 2020;149: 783-793.
21. Cascione M, De Matteis V, Pellegrino P, Albanese G, De Giorgi ML, Paladini F, Corsalini, M, Rinaldi R. Improvement of PMMA dental matrix performance by addition of titanium dioxide nanoparticles and clay nanotubes. *Nanomaterials*. 2021;11(8): 2027.
22. Zhou D, Yuan H, Xiong Y, Luo G, Shen Q. Constructing highly directional multilayer cell structure (HDMCS) towards broadband electromagnetic absorbing performance for CNTs/PMMA nanocomposites foam. *Composites Science and Technology*. 2021;203: 108614.
23. Tripathi SN, Saini P, Gupta D, Choudhary V. Electrical and mechanical properties of PMMA/reduced graphene oxide nanocomposites prepared via in situ polymerization. *Journal of materials science*. 2013;48(18): 6223-6232.
24. Tripathi SN, Saini P, Gupta D, Choudhary V. Electrical and mechanical properties of PMMA/reduced graphene oxide nanocomposites prepared via in situ polymerization. *Journal of materials science*. 2013;48(18): 6223-6232.
25. Al-Osaimi J, Al-Hosiny N, Abdallah S, Badawi A. Characterization of optical, thermal and electrical properties of SWCNTs/PMMA nanocomposite films. *Iranian Polymer Journal*. 2014;23(6): 437-443.
26. Zhang Y, Zhuang S, Xu X, Hu J. Transparent and UV-shielding ZnO@ PMMA nanocomposite films. *Optical Materials*. 2013;36(2): 169-172.
27. Suematsu K, Arimura M, Uchiyama N, Saita S. Transparent $BaTiO_3$/PMMA nanocomposite films for display technologies: facile surface modification approach for BaTiO3 nanoparticles. *ACS Applied Nano Materials*. 2018;1(5): 2430-2437.
28. Li B, Yuan H, Zhang Y. Transparent PMMA-based nanocomposite using electrospun graphene-incorporated PA-6 nanofibers as the reinforcement. *Composites Science and Technology*. 2013;89: 134-141.
29. Pal K. Effect of different nanofillers on mechanical and dynamic behavior of PMMA based nanocomposites. *Composites Communications*. 2016;1: 25-28.
30. Eriksson M, Goossens H, Peijs T. Influence of drying procedure on glass transition temperature of PMMA based nanocomposites. *Nanocomposites*. 2015;1(1): 36-45.

31. Hu H, Bhowmik P, Zhao B, Hamon MA, Itkis ME, Haddon RC. Determination of the acidic sites of purified single-walled carbon nanotubes by acid–base titration. *Chemical Physics Letters*. 2001;345(1-2): 25-28.
32. Hu H, Zhao B, Itkis ME, Haddon RC. Nitric acid purification of single-walled carbon nanotubes. *The Journal of Physical Chemistry B*. 2003;107(50): 13838-13842.

THE AUTHORS

Guo Qin Liu
e-mail: polymerpaper@163.com

Meng Yao Hou
e-mail: liugq1970@126.com

Shuai Qian Wang
e-mail: wangpolymer@163.com